Available online at www.sciencedirect.com

SciVerse ScienceDirect

Ceramics International 38 (2012) 1221–1225

CERAMICS INTERNATIONAL

www.elsevier.com/locate/ceramint

Preparation, characterization and dielectric properties of $CaCu_3Ti_4O_{12}$ ceramics

Jingchang Zhao *, Jia Liu, Guang Ma

Department of Materials Science and Engineering, Yunnan University, Kunming, PR China

Received 25 November 2010; received in revised form 12 July 2011; accepted 28 July 2011
Available online 2 September 2011

Abstract

$CaCu_3Ti_4O_{12}$ nano-sized powders were successfully prepared by sol–gel technique and calcination at 600–900 °C. The thermal decomposition process, phase structures and morphology of synthesized powders were characterized by IR, DSC-TG, XRD, TEM, respectively. It was found that the main weight-loss and decomposition of precursors occurred below 450 °C and the complex perovskite phase appeared when the calcination temperature was higher than 700 °C. Using above synthesized powders as starting materials, CCTO-based ceramics with excellent dielectric properties ($\varepsilon_{25} = 5.9 \times 10^4$, $\tan\delta = 0.06$ at 1.0 kHz) were prepared by sintering at 1125 °C. According to the results, a conduction mechanism was proposed to explain the origin of giant dielectric constant in CCTO system.

Keywords: Dielectric properties; $CaCu_3Ti_4O_{12}$; Sol–gel

1. Introduction

Although many ferroelectric and relaxor ferroelectric materials have been widely used to fabricate capacitors at present [1–3], their dielectric properties are generally closely related to the spontaneous polarization and phase transition, which resulted in a large variation in capacitance and dielectric loss at the Curie temperature, as well as fatigue and ageing problem at an alternating electric field [4,5]. With the development of miniaturization and integration in device manufacture, it is still intriguing to develop a new type of capacitors with higher permittivity and more stable temperature characteristics [6,7].

$CaCu_3Ti_4O_{12}$ (CCTO) is a kind of composite perovskite materials with body-centered cubic structure at room temperature [8], which has received intensive attention because this material in ceramic and single-crystalline forms shows a giant dielectric constant ($>10^5$) with nearly constant over a wide temperature range (100–600 K) [9,10]. Furthermore, as a lead-free system, the sintering temperature of CCTO materials is generally 1050–1150 °C, which is lower than that of some conventional titanate-based ceramics [11]. Owing to above remarkable properties, CCTO is being considered as a very promising material for application in microelectronics, such as dielectric planar antennas, capacitors, *R*//*C* circuit and microwave devices etc. [12,13].

Currently, some hypotheses have been proposed to explain the origin of colossal dielectric constant in CCTO system [14–18], mainly including the extrinsic factors (defects and grain boundaries, etc.) and the intrinsic factors (lattice vibrations, etc.). A model of internal barrier layer capacitor (IBLC) has been widely accepted to describe their microstructures and as the most likely mechanism to elucidate the colossal dielectric constant in CCTO system [19,20]. However, there are still some experimental results cannot be explained reasonably, such as the origin of charges in semiconducting regions, the microstructure of insulating barriers, etc. On the other hand, it has been reported that CCTO-based electroceramics with giant dielectric constant can be fabricated without doping donor oxides and sintering in air atmosphere [21,13]. It shows that the formation mechanism of CCTO-based electroceramics is different from the conventional titanate-based ceramics [22,23]. So it is still necessary to further investigate the electrical properties, microstructure and conduction mechanism of this serial of materials.

---

* Corresponding author.
E-mail address: jchzhao@ynu.edu.cn (J. Zhao).

0272-8842/$36.00 © 2011 Elsevier Ltd and Techna Group S.r.l. All rights reserved.
doi:10.1016/j.ceramint.2011.08.052

2. Experimental

Analytical grade $Ca(NO_3)_2{\cdot}4H_2O$, $Cu(NO_3)_2{\cdot}3H_2O$ and $Ti(OC_4H_9)_4$ were used as the starting materials to synthesize the precursors of $CaCu_3Ti_4O_{12}$ powders. The weighted $Ca(NO_3)_2{\cdot}4H_2O$, $Cu(NO_3)_2{\cdot}3H_2O$ (stoichiometric ratio is 3:1) were dissolved into CH_3CH_2OH and deionize water (3:1 vol%) to form 2.0 M nitrate solution. Amount of acetic acid was added to adjust the acidity of solution (pH = 3) in order to form the gels slowly. Meanwhile, stoichiometric $Ti(OC_4H_9)_4$ liquids were dissolved into CH_3CH_2OH to form 0.5 M solution. Under stirring, both above solutions were mixed slowly at room temperature and the sky-blue gels were gradually formed. Subsequently, the gels were heated for 4 h at 60 °C in a water bath and then dried at 100 °C for 24 h to obtain the dry precursors. Finally, the precursors were calcined at 600–900 °C for 2 h in air to obtain $CaCu_3Ti_4O_{12}$ powders.

Infrared ray (IR) absorption of synthesized $CaCu_3Ti_4O_{12}$ dry precursors was measured from 400 cm^{-1} to 4000 cm^{-1} by using Fourier transform infrared spectrometer (Varican-1000). Thermal decomposition of dry precursors was investigated by thermogravimetric and differential thermal analyses from room temperature to about 800 °C at a heating rate of 10 °C/min by using thermoanalyser (TA SDT2960). The crystalline structures of obtained powders and ceramic were examined by using Regaku D/max IIIB X-ray diffraction meter (Cu $K\alpha_1$). The morphology of 800 °C-calcined powders was observed by HITACHI-800 transmission electron microscope (TEM).

Using conventional ceramic technique, the prepared powders were uniaxially pressed into 10 mm diameter discs of about 1 mm thickness at a pressure of 10^8 Pa. Then, the green pellets were sintered in air at 1125 °C for 4 h to obtain dense ceramics. Silver electrodes were coated on the surface of ceramics and annealed at 800 °C for 10 min. The microstructures of samples were observed by JSM-6301F scanning electron microscope (SEM), and their dielectric properties were measured from −100 °C up to 150 °C by using an impedance analysis system (HP4284A).

3. Results and discussion

FT-IR spectrum of sol–gel synthesized CCTO dry precursor was shown in Fig. 1. It can be seen that a strong and broad absorption band appears in the region of 2800–3600 cm^{-1}, centered at 3447 cm^{-1}, originated from the O–H vibration of weak-bound water, butanol and C–H vibration of alkyl groups in precursors. The characteristic absorption peaks of NO_3^{2-} appear near the wave number 1382 cm^{-1}. The absorption peaks of 1636 cm^{-1}, 1543 cm^{-1} and 1045 cm^{-1} are attributed to the asymmetrical stretching vibration and the symmetrical stretching vibration of $–COO^-$.

Fig. 2 gives the variances of the heat flow and the specimen's gravity from room temperature to about 780 °C. The DSC curve appears a small endothermatic peak at about 120 °C, accompanied by about 10% weight loss in TG curve, which resulted from the removal of weak-bound water and butanol. At the elevating temperature, in the range of 155–450 °C, a strong exothermic peak appears at 275.9 °C, accompanied by more than 48% weight loss in TG curve. The main decomposition of nitrates and organic groups occurred in this temperature range. Above 450 °C, almost no weight loss was found in TG curve, non-crystalline oxides slowly reacted and transferred to polycrystallines.

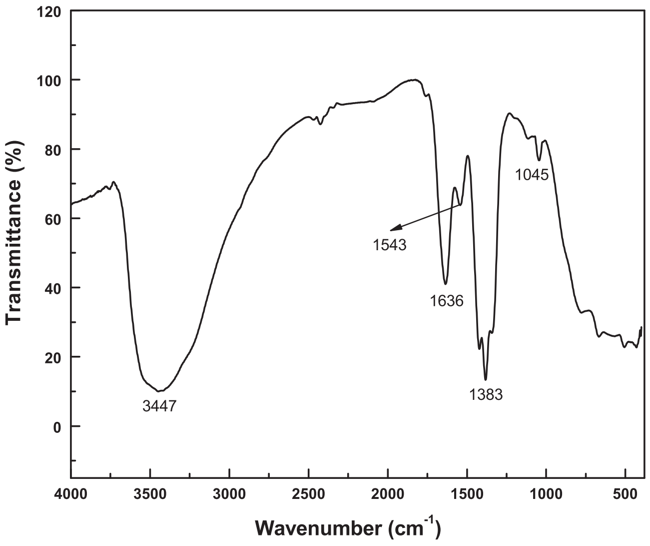

Fig. 1. FT-IR spectrum of sol–gel synthesized CCTO precursors.

XRD patterns of 600–900 °C-calcined CCTO powders were shown in Fig. 3. It can be seen there is almost no CCTO phase formed in 600 °C-calcined powders, only a small amount of CuO and anatase TiO_2 were observed. With increasing the calcinations temperature from 600 °C to 900 °C, the diffraction peaks corresponding CCTO crystalline gradually appeared and became stronger. On the contrary, the content of CuO and TiO_2 gradually decreased and anatase TiO_2 gradually disappeared and transferred to rutile phase. When the calcinations temperature reached 900 °C, impurity phases (CuO and TiO_2) completely disappeared and pure CCTO powders with cubic structure were obtained, the corresponding crystalline indexes were marked in Fig. 3.

The morphology of 800 °C-calcined CCTO powders is shown in Fig. 4. It can be seen that the sizes of most particles are

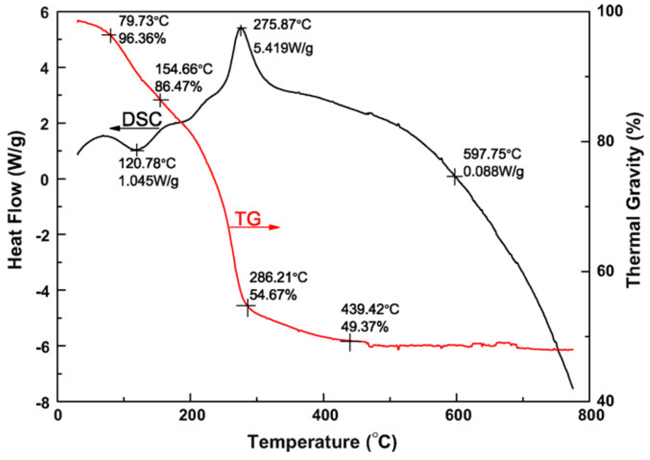

Fig. 2. DSC/TG curves of sol–gel synthesized CCTO precursors.

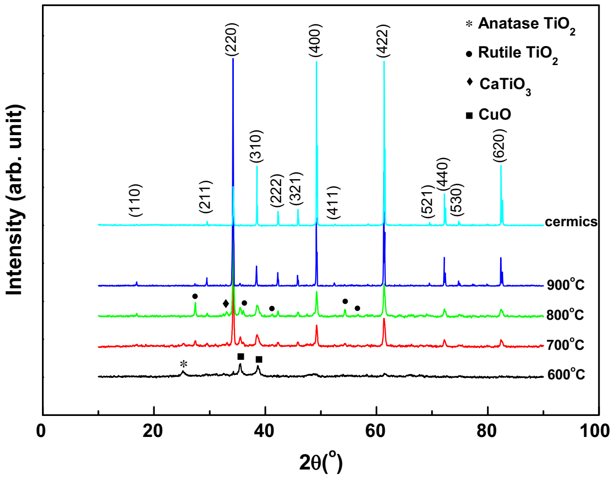

Fig. 3. XRD patterns of 600–900 °C–2 h calcined CCTO powders and 1125 °C–4 h sintered CCTO ceramic.

less than 100 nm and some ultrafine particles can be observed at the corner region.

The dependences of dielectric constant and dielectric loss on the temperatures are shown in Fig. 5(a and b), respectively. It can be seen that the sample exhibits a high dielectric constant ($\varepsilon_{25} = 5.9 \times 10^4$, 1.0 kHz) and low dielectric loss ($\tan \delta = 0.06$, 1.0 kHz) at room temperature, as well as a stable temperature characteristics. With increasing measuring frequencies, sample's dielectric constant gradually decreased and the range with stable temperature characteristics moved to high temperature.

Fig. 6(a and b) gives the morphologies of 1125 °C–4 h sintered sample's surface and fracture, respectively. The sizes of most grains on the ceramic surface are in the range of 20–50 μm. The large grains on the fracture contain pores indicative of fast grain growth. Some small particles and deposits can be observed at the grain junctions, which might resulted from the decomposition of partial CCTO and segregation of oxides during the sintering at high temperature. The previous investigation of EDS revealed that the doped or undoped CCTO ceramics present well-defined grain boundaries, rich in

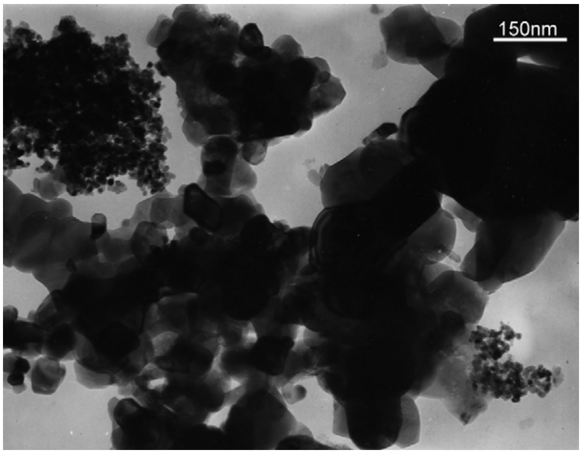

Fig. 4. TEM micrography of sol–gel synthesized CCTO powders calcined at 800 °C for 2 h.

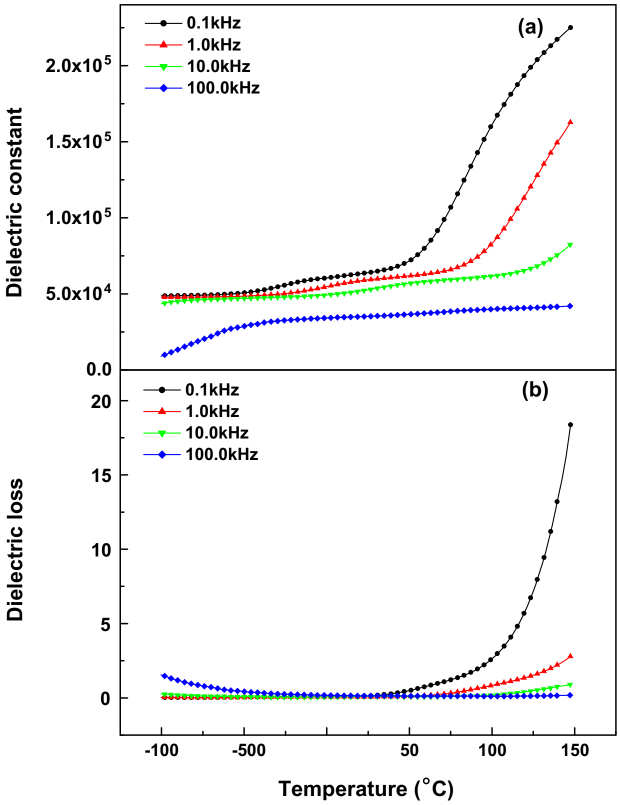

Fig. 5. ε–T (a) and D–T (b) curves of 1125 °C–4 h sintered CCTO ceramics.

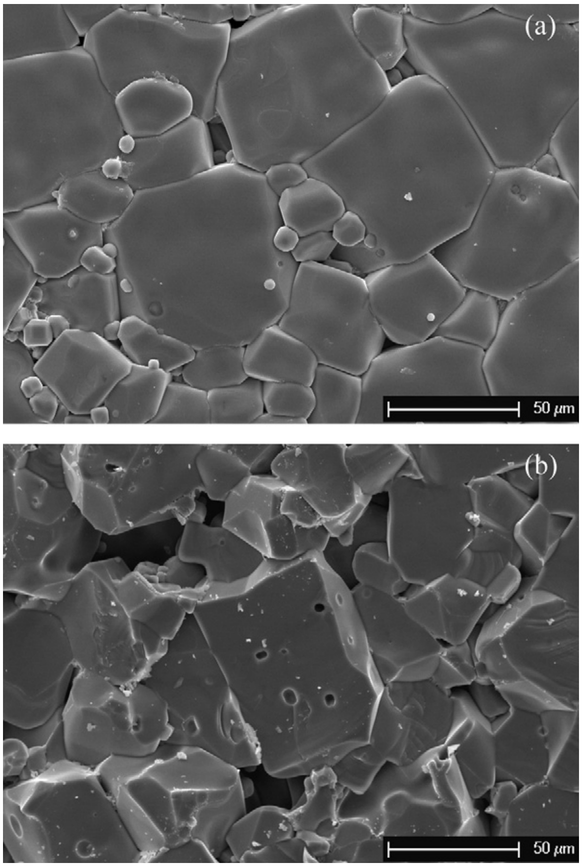

Fig. 6. SEM micrograph of 1125 °C–4 h sintered CCTO ceramics: (a) surface, (b) fracture.

Cu and deficient in Ca and Ti, forming a microstructure in which each grain is surrounded by exfoliated sheets of Cu-rich phase [10,13]. On the other hand, the sintered ceramics mainly ruptured along the grain boundaries in Fig. 6(b), it confirms that the strength of grain interiors is higher than that of grain boundaries.

TiO_2-based semiconducting ceramics, such as $BaTiO_3$, $SrTiO_3$, generally have the microstructure of semiconducting grains and isolation grain boundaries [22,23]. The formation of oxygen vacancies $V_O^{\bullet\bullet}$ in reducing atmosphere or donor defects through replacing A or Ti positions by high-valence donors resulted in the formation of n-type semiconducting grains, their corresponding electrical properties originate from the double Schottky barriers, which caused by a depletion of the mobile carriers in the vicinity of the grain boundary. As to CCTO system, although it also has the microstructure of semiconducting grains and isolation grain boundaries, the origin of charges is different from the common perovskite materials. Li et al. [14], proposed a cation non-stoichiometry model to explain the origin of giant dielectric constant in CCTO system. The reduction of divalent Cu ions at sintering stage and re-oxidation of monovalent Cu ions at cooling stage resulted in a charge balance substitution of Ti^{4+} on the Cu site as well as the reduction of Ti^{4+} to Ti^{3+}. The recent XPS results also confirmed that Cu^+ and Ti^{3+} ions exist in CCTO dielectric ceramics [9]. However, during sintering CCTO-based ceramics in an oxiding atmosphere, it is difficult to produce oxygen vacancies $V_O^{\bullet\bullet}$ because of the high oxygen pressure. As a result, Cu ions in the grain interiors will not change from divalence to monovalence at this stage considering the charge balance. On the other hand, CCTO is easy to decompose at high sintering temperature. Some CuO will leave lattices to segregate on the grain boundaries or to volatize into air. After Cu^{2+} ions leaving lattices, the defects V''_{Cu} with negative charges need to be compensated by other defects with positive charges. Furthermore, the radius of Cu^{2+} ions ($r_{Cu^{2+}} = 0.72$ Å) is close to the radius of Ti^{4+} ions ($r_{Ti^{4+}} = 0.68$ Å), but much smaller than the radius of Ca^{2+} ions ($r_{Sr^{2+}} = 0.99$ Å). Therefore, it is assumed that Ti^{4+} ions would preferentially occupy Cu^{2+} positions in CCTO lattices to form donor defects $Ti_{Cu}^{\bullet\bullet}$. The residual positive charge will be compensated by valence change of other Ti^{4+} or Cu^{2+} ions. The possible process can be described as following:

$$\begin{aligned}&CaCu_3Ti_4O_{12} + xTi_{Ti}\\&\quad + \tfrac{x}{2}O_2 \rightarrow Ca^{2+}(Cu^{2+}_{3-x}Ti^{4x}_{x})(Ti^{4+}_{4-2x}Ti^{3+}_{2x})O_{12} + xCuO \end{aligned} \tag{1}$$

$$\begin{aligned}&CaCu_3Ti_4O_{12} + xTi_{Ti}\\&\quad + \tfrac{x}{2}O_2 \rightarrow Ca^{2+}(Cu^{2+}_{3-3x}Cu^{1+}_{2x}Ti^{4+}_{x})Ti^{4+}_{4}O_{12} + xCuO \end{aligned} \tag{2}$$

Eqs. (1) and (2) represent the donor defects $Ti_{Cu}^{\bullet\bullet}$ are compensated by valence change of partial Ti^{4+} and Cu^{2+} ions, respectively. The hopping of charges between Ti sites and Cu sites increases the concentration and movability of charges in the grains, which results in a high electrical conduction of this serial of n-type semiconducting ceramics. According to above defect equations, CuO loss from lattices plays a key role to obtain giant dielectric constant CCTO-based electroceramics. It is estimated that decomposition of CCTO would produce vacancies of copper ions, which is beneficial to the substitution of Cu positions by Ti ions at the high temperature. Certainly, the decomposed CuO will volatize into air or segregate on the grain boundaries, where divalent Cu^{2+} can also be reduced to monovalent Cu^+ ions at high sintering temperature.

Based on simple brick wall model [24], the effective permittivity (ε_{eff}) of IBLC is in proportion to the ratio of the average grain size (d_{gr}) and the grain boundary depletion layer width (d_{gb}), as well as the permittivity in grain boundary layer (ε_{gb}):

$$\varepsilon_{eff} = \varepsilon_{gb}\frac{d_{gr}}{d_{gb}} \tag{3}$$

Therefore, it is important for fabricating IBLC to obtain the grain boundaries with proper width, good isolation and high dielectric constant. As for CCTO dielectric ceramics, CuO leaves lattices and deposits on the grain boundaries to form a high-quality isolation layer, which is helpful to the increase of capacitance. However, if overmuch CuO leaves lattices and segregates on the grain boundaries, the thickness of grain boundaries depletion layer would increase and the vacancies of Cu ions could not be completely occupied by Ti ions. As a result, some acceptor defects V''_{Cu} would combine with donor defects $Ti_{Cu}^{\bullet\bullet}$ to form complex defects $(Ti_{Cu}^{\bullet\bullet}V''_{Cu})$, which perhaps weaken the effect of substitution of Cu positions by Ti ions and decrease the grain conduction of CCTO-based ceramics.

4. Conclusions

In this paper, sol–gel route was employed to synthesize CCTO nano-size powders. The investigation of DSC/TG, XRD showed that the main weight-loss and decomposition of precursors occurred below 450 °C, and CCTO crystalline gradually appeared and became stronger when the calcination temperature was higher than 700 °C. Using sol–gel synthesized powders as starting materials, CCTO-based ceramics with excellent dielectric properties were obtained by sintering in air at 1125 °C. Sample's permittivity gradually decreased and the range with stable temperature characteristics moved to high temperature with increasing measuring frequency.

CuO loss from lattices plays a key role to obtain giant dielectric constant in CCTO-based electroceramics. It is assumed that Ti^{4+} ions would preferentially occupy Cu^{2+} positions in CCTO lattices to form donor defects $Ti_{Cu}^{\bullet\bullet}$. The residual positive charge could be compensated by valence change of other Ti^{4+} or Cu^{2+} ions, which resulted in the giant dielectric constant of CCTO-based ceramics.

Acknowledgments

The authors are grateful to the financial supports from Natural Science Foundation of Yunnan Province (no. 2007E024M) and Major Teacher Training Foundation of Yunnan University of China.

References

[1] H. Kishi, Y. Mizuno, H. Chazono, Base-metal electrode-multilayer ceramic capacitors: past, present and future perspectives, Jpn. J. Appl. Phys. 42 (2003) 1–15.

[2] V. Koval, C. Alemany, J. Briancin, H. Brunckova, Dielectric properties and phase transition behavior of xPMN-$(1-x)$PZT ceramic systems, J. Electroceram. 10 (2003) 19–29.

[3] J.W. Zhai, X. Yao, H. Chen, Structural and dielectric properties of $Ba_{0.85}Sr_{0.15}(Zr_{0.18}Ti_{0.85})O_3$ thin films grown by a sol–gel process, Ceram. Int. 30 (2004) 1237–1240.

[4] O. Auciello, S. Saha, D.Y. Kaufman, S.K. Streiffer, et al., Science and technology of high dielectric constant thin films and materials integration for application to high frequency devices, J. Electroceram. 12 (2004) 119–131.

[5] A. Sidorkin, L. Nesterenko, A. Sidorkin, S. Ryabtsev, G. Bulavina, Ageing and fatigue of lead titanate and lead zirconate titanate thin ferroelectric films, Solid State Sci. 12 (2010) 302–306.

[6] H. Shen, Y.W. Song, H. Gu, P.C. Wang, Y.M. Xi, A high-permittivity $SrTiO_3$-based grain boundary barrier layer capacitor material single-fired under low temperature, Mater. Lett. 56 (2002) 802–805.

[7] J.Z. Zhao, X.H. Wu, L.T. Li, X. Li, Preparation and electrical properties of $SrTiO_3$ ceramics doped with M_2O_3–PbO–CuO, Solid State Electron. 48 (2004) 2287–2291.

[8] C.C. Homes, T. Vogt, S.M. Shapiro, Charge transfer in the high dielectric constant materials $CaCu_3Ti_4O_{12}$ and $CdCu_3Ti_4O_{12}$, Phys. Rev. B 67 (2003) 092106.

[9] L. Ni, X.M. Chen, Dielectric relaxations and formation mechanism of giant dielectric constant step in $CaCu_3Ti_4O_{12}$ ceramics, Appl. Phys. Lett. 91 (2007) 122905.

[10] F. Amaral, C.P.L. Rubinger, M.A. Valente, et al., Enhanced dielectric response of GeO_2-doped $CaCu_3Ti_4O_{12}$ ceramics, J. Appl. Phys. 105 (2009) 034109.

[11] D.F.K. Hennings, Dielectric materials for sintering in reducing atmospheres, J. Eur. Ceram. Soc. 21 (2001) 1637–1642.

[12] L.C. Kretly, A.F.L. Almeida, P.B.A. Fechine, R.S. De Oliveira, A.S.B. Sombra, Dielectric permittivity and loss of $CaCu_3Ti_4O_{12}$(CCTO) substrates for microwave devices and antennas, J. Mater. Sci. Mater. Electron. 15 (2004) 657–663.

[13] B.A. Bender, M.-J. Pan, The effect of processing on the giant dielectric properties of $CaCu_3Ti_4O_{12}$, Mater. Sci. Eng. B 117 (2005) 339–347.

[14] J. Li, M.A. Subramanian, H.D. Rosenfeld, C.Y. Jones, B.H. Toby, A.W. Sleight, Clues to the giant dielectric constant of $CaCu_3Ti_4O_{12}$ in the defect structure of $SrCu_3Ti_4O_{12}$, Chem. Mater. 16 (2004) 5223–5225.

[15] A. Tselev, C.M. Brooks, S.M. Anlage, et al., Evidence for power-law frequency dependence of intrinsic dielectric response in the $CaCu_3Ti_4O_{12}$, Phys. Rev. B 70 (2004) 144101.

[16] M.H. Cohen, J.B. Neaton, L.X. He, D. Vanderbilt, Extrinsic models for the dielectric response of $CaCu_3Ti_4O_{12}$, J. Appl. Phys. 94 (5) (2003) 3299–3306.

[17] D. Valim, A.G. Souza, P.T.C. Freire, et al., Raman scattering and X-ray diffraction studies of polycrystalline $CaCu_3Ti_4O_{12}$ under high-pressure, Phys. Rev. B 70 (2004) 132103.

[18] P. Lunkenheimer, R. Fichtl, S.G. Ebbinghaus, A. Loidl, Nonintrinsic origin of the colossal dielectric constants in $CaCu_3Ti_4O_{12}$, Phys. Rev. B 70 (2004) 172102.

[19] S. Kwon, C.C. Huang, M.A. Subramanian, D.P. Cann, Effects of cation stoichiometry on the dielectric properties of $CaCu_3Ti_4O_{12}$, J. Alloys Compd. 473 (2009) 433–436.

[20] A.R. West, T.B. Adams, F.D. Morrison F.D, et al., Novel high capacitance materials: $BaTiO_3$:La and $CaCu_3Ti_4O_{12}$, J. Eur. Ceram. Soc. 24 (6) (2004) 1439–1448.

[21] G. Chiodelli, V. Massarotti, D. Capsoni, et al., Electric and dielectric properties of pure and doped $CaCu_3Ti_4O_{12}$ perovskite materials, Solid State Commun. 132 (3–4) (2004) 241–246.

[22] F.D. Morrison, A.M. Coats, D.C. Sinclair, A.R. West, Charge compensation mechanisms in La-doped $BaTiO_3$, J. Electroceram. 6 (2001) 219–232.

[23] J.H. Hwang, Y.H. Han, Defect chemistry of Er-doped $BaTiO_3$, Solid State Ionics 140 (2001) 181–186.

[24] R. Waser, Electronic properties of grain boundaries in $SrTiO_3$ and $BaTiO_3$ ceramics, Solid State Ionics 75 (1995) 89–99.